presented at ASME Int. Gas Turbine and Aeroengine Congress, Orlando, 1997 as paper 97-GT-136

HEAT TRANSFER IN A ROTATING CAVITY WITH A PERIPHERAL INFLOW AND OUTFLOW OF COOLING AIR

Iraj Mirzaee, Xiaopeng Gan*, Michael Wilson and J Michael Owen

School of Mechanical Engineering
University of Bath
Bath BA2 7AY, UK

ABSTRACT

This paper describes a combined computational and experimental study of the heat transfer in a rotating cavity with a peripheral inflow and outflow of cooling air for a range of rotational speeds and flow rates. Measurements are made in a purpose-built rig, with one of the two rotating discs heated, and computations are conducted using an axisymmetric elliptic solver incorporating the Launder-Sharma low-Reynolds-number k-ε turbulence model. Measured values of the tangential component of velocity, V_ϕ, exhibit Rankine-vortex behaviour which is not accurately modelled by the computations. Both computed and measured values of the radial component of velocity, V_r, confirm the recirculating nature of the flow. In the outflow region, agreement between computed and measured values of V_r is mainly good, but in the inflow region the computations exhibit a "peaky" distribution which is not shown by the measurements. The measured and computed Nusselt numbers show that Nu increases as the magnitudes of the flow rate and the rotational speed increase. The computed Nusselt numbers (allowing for the effects of conduction through and radiation to the unheated disc) reproduce the measured trends but tend to underestimate the experimental values at the larger radii.

* *Now at European Gas Turbines Ltd, Whetstone, Leicester LE8 6LH, UK*

NOMENCLATURE

a, b	inner, outer radius of disc
A, B	constants in equation (1)
$C_{\varepsilon 2}$	turbulence model coefficient (Appendix A)
C_{gs}	correction coefficient (Appendix A
C_w	nondimensional mass flow rate (=m/μb)
G	gap ratio (= s/b)
h	heat transfer coefficient
k	turbulent kinetic energy, thermal conductivity
m	mass flow rate
Nu	Nusselt number ($Nu = qr/k(T_s - T_{ref})$)
q	heat flux from heated disc to air
r	radial coordinate
Re_ϕ	rotational Reynolds number ($=\rho\Omega b^2/\mu$)
Ri_{gs}	Richardson-number (Appendix A)
s	axial gap between discs
T	static temperature
U_τ	friction velocity ($=\sqrt{(\tau_w/\rho)}$)
V_r, V_ϕ, V_z	time-averaged velocities in r, ϕ, z directions
x	nondimensional radius (=r/b)
y	distance normal to wall
y+	wall-distance Reynolds number ($= \rho U_\tau y/\mu$)
z	axial coordinate
ε	turbulent energy dissipation rate
λ_T	turbulent flow parameter ($= C_w Re_\phi^{-0.8}$)
μ	dynamic viscosity
ρ	density
ϕ	tangential coordinate
τ_w	total wall shear stress
Ω	angular speed of discs

Subscripts

eff	effective value
fd	free-disc value
s	disc surface
ref	reference value

1 INTRODUCTION

In some gas-turbine designs, the cooling air for the rotating turbine discs is supplied through a stationary casing at the periphery of the discs, as shown in Fig 1. The air enters the annular rotating cavity between the discs through nozzles in the stationary casing and leaves through the small clearances between the discs and the casing.

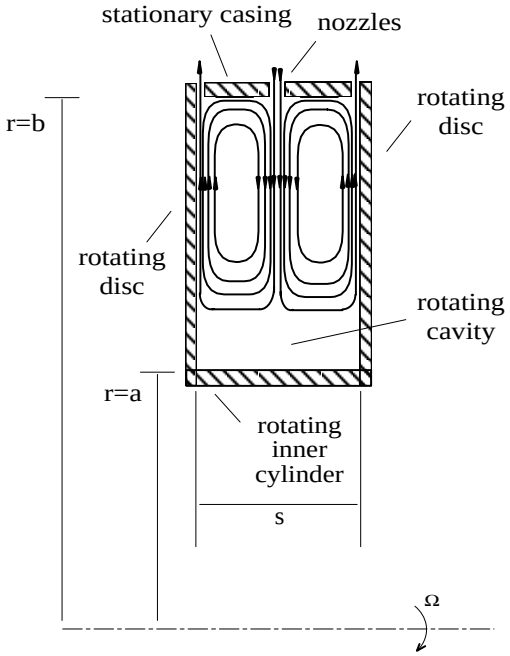

Fig. 1 Rotating cavity with a peripheral flow of cooling air

A combined computational and experimental study of the turbulent flow in this system was conducted by Gan *et al* (1996), and some of the computed streamlines are shown in Fig 2. The computations are shown for rotational Reynolds numbers of Re_ϕ = 3.75 x 10^5 and 1.5 x 10^6, and for nondimensional flowrates of C_w = -1500 and -3000, where the negative sign is used to indicate that the inlet flow is radially inward. The four cases correspond to values of the turbulent flow parameter, λ_T, between -0.0172 and -0.104, which are representative of the values used in the internal cooling-air systems of engines. (For a free disc, the nondimensional flow rate entrained by one side of the disc, $C_{w,fd}$, is given by $C_{w,fd} = 0.219\ Re_\phi^{0.8}$; a value of $|\lambda_T| = 0.219$ therefore corresponds to the free-disc entrainment rate. Further discussion of the turbulent flow parameter is given by Owen and Rogers 1989, 1995.) For the computations, the flow entered the system radially, without swirl, in the mid-plane (z/s = 0.5); the outlet flow was split equally between the clearances at z = 0 and z = s. The gap ratio was G = 0.30, and the inner-to-outer radius ratio was a/b = 0.5.

It can be seen from Fig 2 that there is recirculating flow, symmetrical about the mid-plane. The radial extent of the recirculation zone, which increases as $|\lambda_T|$ increases, is governed by two effects: (i) the shear exerted by the stationary peripheral casing on the rotating air in the cavity; (ii) the exchange of angular momentum between the incoming air and the rotating air.

Computations and measurements of the velocity showed that there is radial outflow in thin boundary layers on the disc and radial inflow in the core between the boundary layers. In the core, the tangential component of velocity, V_ϕ, is invariant with z, and the measured values of V_ϕ conform to a combined free and forced vortex, or Rankine vortex (see Owen and Rogers 1995), where

$$\frac{V_\phi}{\Omega r} = Ax^{-2} + B \qquad (1)$$

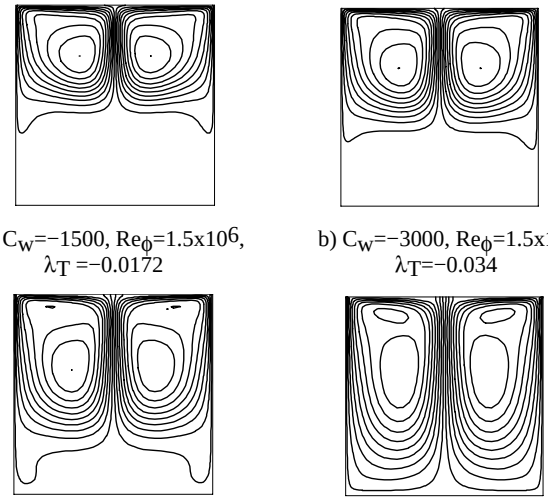

a) C_w=−1500, Re_ϕ=1.5x10^6, λ_T =−0.0172

b) C_w=−3000, Re_ϕ=1.5x10^6, λ_T=−0.034

c) C_w=−1500, Re_ϕ=3.75x10^5, λ_T =−0.052

d) C_w=−3000, Re_ϕ=3.75x10^5, λ_T=−0.104

Fig. 2 Computed streamlines (from Gan et al 1996)

and the coefficients A and B depend on C_w and Re_ϕ. The computations were unable to capture this Rankine-vortex behaviour; deficiencies in the turbulence model were believed to be responsible.

This paper describes a combined computational and experimental study of heat transfer in the system described above. In addition, a modified version of the turbulence model is used to obtain improved computations of the velocity, and these are compared with measurements of V_ϕ / Ωr. The experimental apparatus is described in Section 2 and the computational method in Section 3. Comparisons between the computations and measurements are given in Section 4, and the conclusions are presented in Section 5.

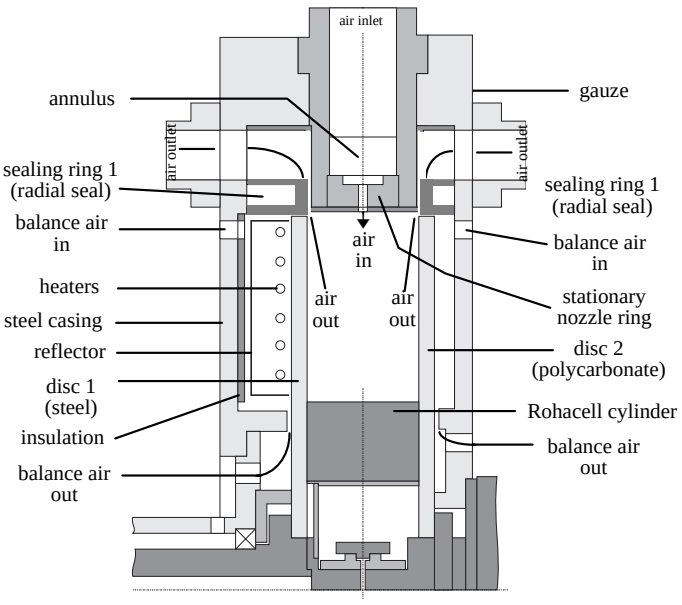

Fig. 3 Rotating cavity rig (from Gan et al (1996))

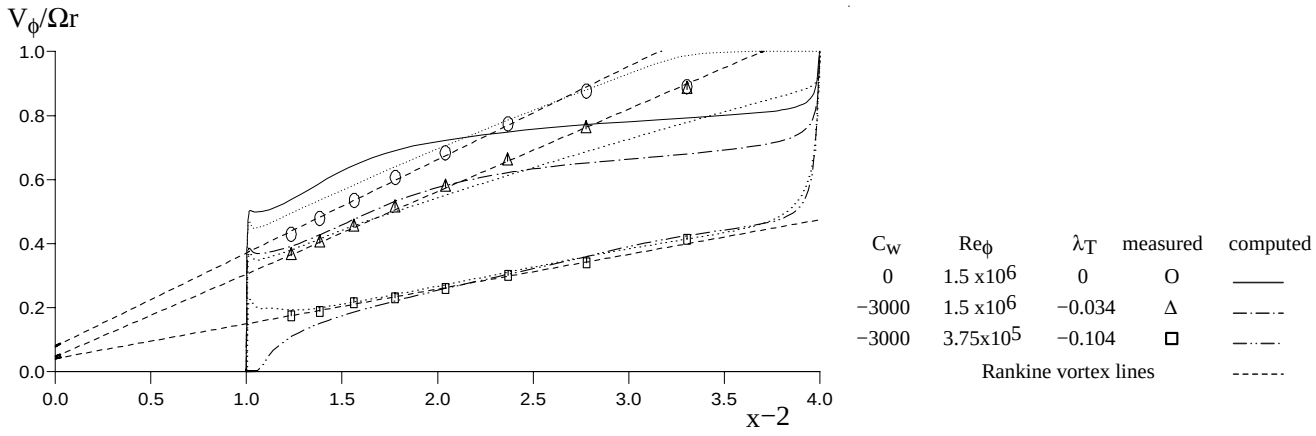

Fig. 4 Variation of $V_\phi/\Omega r$ with x^{-2} for z/s=0.8

····· Launder−Sharma model with Richardson−number correction

2 EXPERIMENTAL APPARATUS

A simple diagram of the rotating-disc rig is shown in Fig 3. Details of the apparatus and instrumentation used for the velocity measurements are given by Gan *et al* (1996) and only the salient features of the rig and details of the heat-transfer instrumentation are described here.

The discs were 762 mm in diameter spaced an axial distance of 113 mm apart (G = 0.30), and the inner cylinder was 382 mm in diameter (a/b = 0.5). Disc 1, which could be heated, was made from steel, and disc 2, which provided optical access for the LDA measurements, was made from transparent polycarbonate. The surfaces of the outer stationary casing and the inner rotating cylinder were insulated with Rohacell, a lightweight foam with a thermal conductivity of k ≅ 0.03 W/mK. The discs and inner cylinder could be rotated up to 1500 rev/min by a 15kW thyristor-controlled electric motor.

The back face of disc 1 was heated to around 100°C by thyristor-controlled stationary radiant heaters with a total output up to 21kW. The front face was coated with a fibre-glass mat, 1mm thick, that contained ten thermocouples and ten fluxmeters. This instrumented disc had been calibrated and tested by Gan *et al* (1995) in their experiments on contra-rotating discs, and the interested reader is referred to that paper for further details. The signals from the thermocouples and fluxmeters were taken out through a silver/silver graphite slipring unit, and the voltages were measured by a computer-controlled data-logger and digital voltmeter with a resolution of ± 1μV.

Air was supplied to the cavity through 39 equi-spaced nozzles of 11.3mm diameter, the axis of each nozzle being on a radial line in the mid-plane of the cavity. The air left the system symmetrically through the two clearances between the stationary casing and the rotating discs; each radial clearance was approximately 1mm. The inlet and outlet flowrates were measured by orifice plates made to British Standards (BS 1042). The difference between the measured inlet flowrate and the sum of the two outlet flowrates was less than 6% of the inlet value.

For the velocity measurements made by Gan *et al* (1996), the roughness of the Rohacell layer on the inner and outer cylindrical surfaces was believed to be a possible contributory factor in the poor agreement between the computed and measured values of $V_\phi/\Omega r$. For those tests, the average roughness of the Rohacell was approximately 30 μm. In later tests, the roughness of the outer cylindrical surface was reduced by coating the Rohacell with varnish, which was subsequently polished; this reduced the average roughness to 8 μm. (Computational results were used to confirm that the thickness of the viscous sublayer was less than 8 μm, so that the varnished surface was considered to be "aerodynamically smooth".) The velocity measurements described below were made with the (new) smooth surfaces, but the heat transfer measurements were made with the (original) rough surfaces.

3 COMPUTATIONAL MODEL

Computations were carried out using an axisymmetric elliptic multigrid solver, incorporating the Launder-Sharma low-Reynolds-number k-ε turbulence model. Incompressible, steady flow was assumed, and full details of the primitive-variables solution were given by Wilson, Pilbrow and Owen (1995). Gan et al (1996) described the computational model used to study the fluid dynamics of the peripheral flow problem. The same model was used for the present work, and only a brief summary will be given in addition to a description of the thermal model. Gan et al (1996) noted that the prediction of tangential velocity distributions might be improved by the use of a Richardson-number based correction to the k-ε turbulence model. A correction of this type is described in Appendix A, and results from the basic and modified models are presented in section 4.

A polynomial fit to measured temperatures was used to provide the radial temperature distribution of the heated disc for each case, and the insulated cylindrical surfaces were assumed to be adiabatic. As the unheated polycarbonate disc provided optical access for the LDA measurements, it could not be insulated and its temperature was not measured. The interior (cavity-side) surface temperature of the polycarbonate disc was estimated by calculating the heat flux through the disc, assuming that its exterior face behaved as a free disc. This was believed to be representative of conditions in the rig, and details of this calculation are given in Appendix B. The influence of the unheated disc temperature on computed Nusselt numbers was investigated by repeating each calculation with an adiabatic assumption for the disc. The results are discussed in section 4.

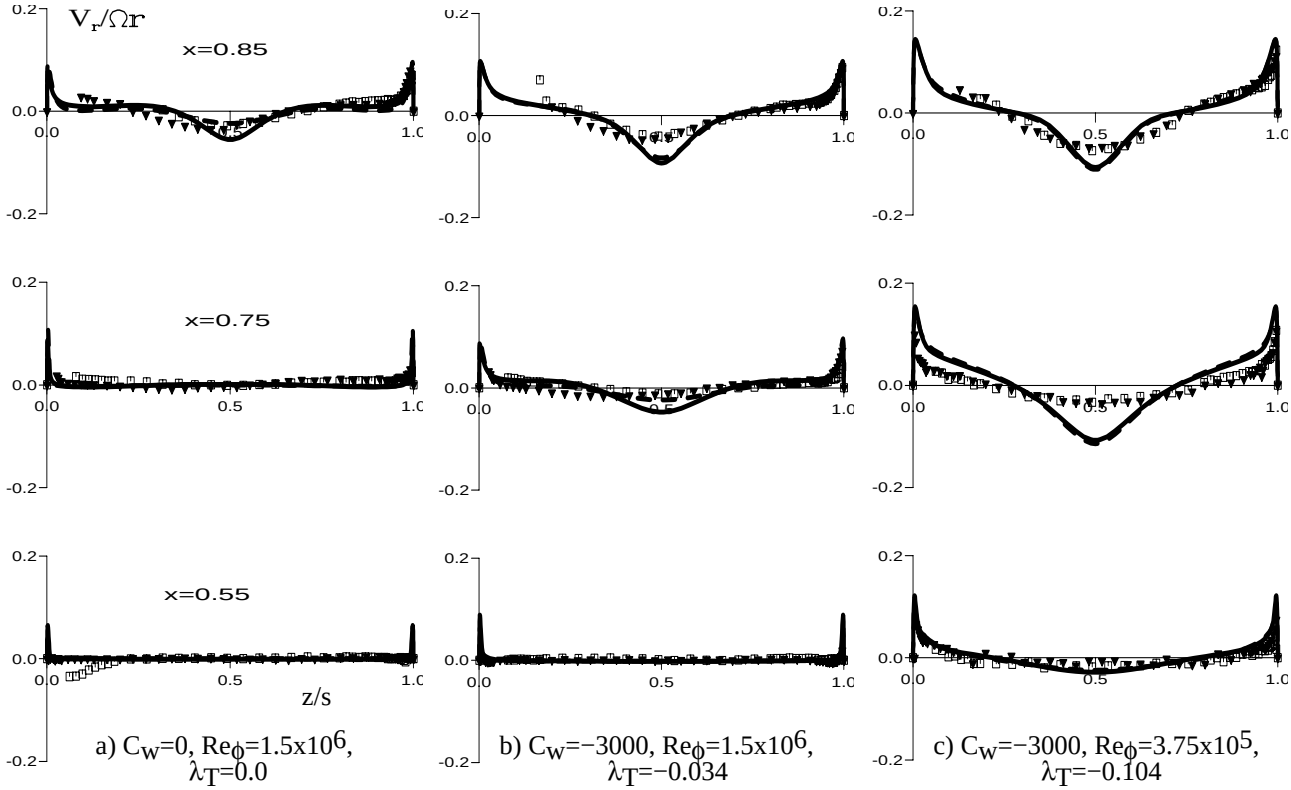

Fig. 5 Variation of $V_r/\Omega r$ with z/s

□ Measured (smooth outer casing)
—— Computed, without Richardson number correcttion

▼ Measured (rough outer casing)
— — - Computed, with Richardson number correcttion

The disc speed, inlet mass flow rate and inlet air temperature were all prescribed from experimental data. A circumferential slot in the outer casing was used to represent the cooling air inlet in the computational model. The slot was located midway between the discs and matched the flow area of the inlet nozzles in the rig. The air entered the system with uniform radial velocity, and the axial and tangential velocity components were zero. The mass flow rates out of the system, at the clearances adjacent to the top of each disc, were equal, and a uniform radial velocity was imposed to ensure mass balance between the inflow and outflows. Zero normal derivative conditions were applied for other variables. No-slip boundary conditions were used for the velocity components parallel to walls. The 89 x 89 axial by radial grid was the same as that described by Gan et al (1996).

The measured disc heat transfer rates include the radiative heat flux between the heated disc and other surfaces (the inner and outer cylinders and the unheated disc). In earlier work, Chen et al (1995) estimated the radiative flux by assuming that the unheated disc was at the inlet temperature of the cooling air, and corrected the measured Nusselt numbers for comparison with convective heat transfer predictions. In the present work, a surface-to-surface radiation model was included in the computations, so that predictions of total Nusselt numbers (including both convective and radiative heat flux) could be compared directly with the measurements. All the surfaces were treated as opaque, grey and diffuse, with temperatures taken from the convective heat transfer predictions. The radiation model is described in detail by Karabay (1996).

4 COMPARISON BETWEEN COMPUTATION AND EXPERIMENT

4.1 Velocity distributions

Fig 4 shows the variation of $V_\phi/\Omega r$ with x^{-2}. On these axes, a straight line represents a Rankine vortex, see equation (1). It can be seen that the experimental data (which were obtained for a "smooth" casing) are closely approximated by equation (1); this was also the case for the data obtained by Gan *et al* (1996) for the "rough" casing. The basic Launder-Sharma model fails to capture the Rankine-vortex behaviour, particularly at smaller values of $|\lambda_T|$. The Richardson correction, discussed in Section 3, produces some improvements but the agreement between computations and experiment cannot be regarded as good.

Fig 5 shows the variation of $V_r/\Omega r$ with z/s for three different cases. The experimental data for the "rough" and "smooth" casings are shown together with the computations with and without the Richardson correction. It can be seen that roughness has comparatively little effect on the measured values of V_r and that the Richardson correction has little effect on the computed values. Both computations and measurements show that there is radial outflow in thin boundary layers on the discs and inflow in the core between the boundary layers. The strength of the recirculation, as denoted by the magnitude of $V_r/\Omega r$, decreases as x decreases.

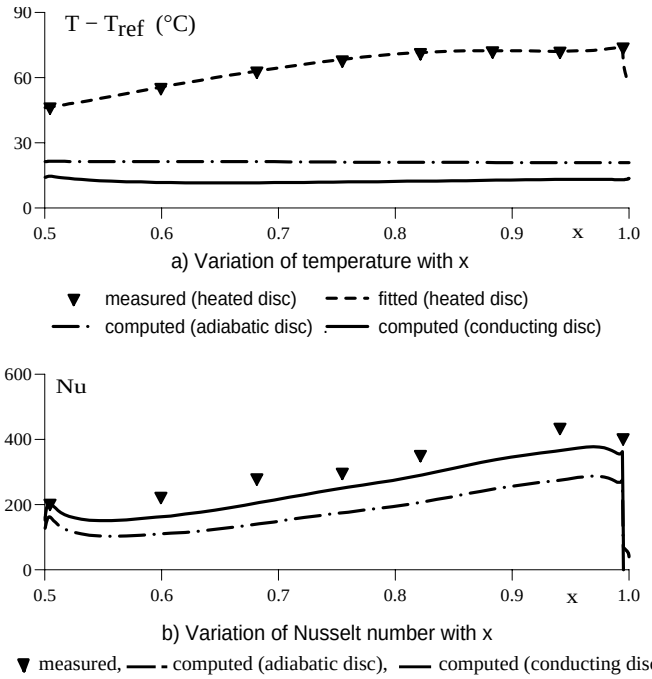

Fig. 6 Variation of temperatures and Nusselt numbers with x: $C_w = -1500$, $Re_\phi = 3.75 \times 10^5$, $\lambda_T = -0.052$

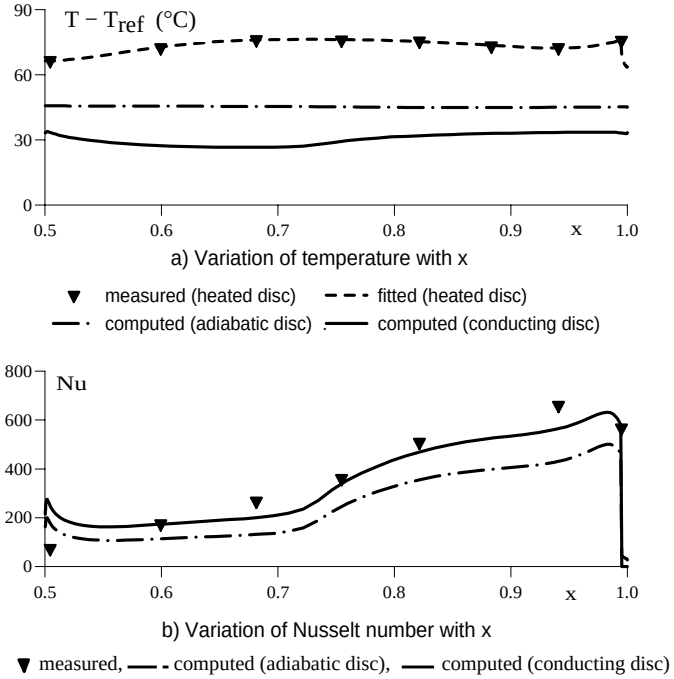

Fig. 7 Variation of temperatures and Nusselt numbers with x: $C_w = -1500$, $Re_\phi = 1.5 \times 10^6$, $\lambda_T = -0.017$

For the results in Fig 5a, where $C_w = 0$, the agreement between the computations and measurements is reasonable. For Figs 5b and 5c, where $|C_w| > 0$, the agreement between the computations and the measurements for radial outflow is mainly good, but the computed radial inflow exhibits a "peaky" distribution that is not shown in the measurements. It should be remembered that the computations are for axisymmetric flow, and the air enters the system through a circular slot in the centre of the stationary casing. In the experiments, the air enters through discrete holes, which may increase mixing and reduce the "peakiness" shown by the computations. It is also possible that the computed peakiness may be caused by deficiencies in the turbulence model.

The measured radial velocity profiles at x = 0.85 and x = 0.75 show some asymmetry for $\lambda_T = 0$ and $\lambda_T = -0.034$ (see Fig 5a, b). Additional computational work has suggested that the radial inflow tends to be unstable at these conditions, giving rise to unsteady flow. The highest flow rate case, $|\lambda_T| = 0.104$, is more symmetrical (see Fig 5c).

4.2 Heat transfer results

Figs 6 to 9 show the computed and measured variations of temperatures and Nusselt numbers with the nondimensional radius x. T_{ref} was taken to be the measured air temperature at inlet to the system.

Fig 6 shows the results for $C_w = -1500$, $Re_\phi = 3.75 \times 10^5$, $\lambda_T = -0.052$. The variation of temperature with x is shown in Fig 6a and the Nusselt numbers in Fig 6b. Referring to Fig 6a, the fitted temperatures on the heated disc were used as boundary conditions for the numerical solution of the energy equation, as discussed in Section 3. For the unheated disc, two assumptions were used : (i) the disc was assumed to be adiabatic; (ii) the disc was assumed to be conducting, with radiation from the heated to the unheated discs.

Fig 6a shows that the temperature of the "conducting disc" is lower than that of the "adiabatic disc", and Fig 6b shows that the "conducting-disc" assumption causes a significant increase in the Nusselt numbers on the heated disc. The increased heat flux from the heated disc occurs as a result of both increased convection to a cooler fluid and radiation from the heated to the unheated disc. (Radiation, which was not included in the adiabatic-disc case, accounts for most of the increased heat flux for the conducting-disc case in Figs 6 to 9.) The computed Nusselt numbers for the conducting-disc case are slightly lower than, but show a similar distribution to, the measured values.

Fig 7 shows the results for $C_w = -1500$, $Re_\phi = 1.5 \times 10^6$, $\lambda_T = -0.017$: the flow rate is the same as for Fig 6 but the rotational speed is higher. The agreement between the computed values of Nu (for the conducting-disc case) and the measured values is reasonable although the computations tend to underestimate the measurements, particularly at the larger values of x. Comparing Figs 6 and 7, it can be seen that increasing Re_ϕ causes an increase in the magnitude of Nu over most of the disc.

Fig 8 shows the results for $C_w = -3000$, $Re_\phi = 3.75 \times 10^5$, $\lambda_T = -0.104$: the rotational speed is the same as for Fig 6 but the flow rate is higher. Again, the computed values of Nu tend to underestimate the measured values, particularly at the larger values of x. Comparing Figs 6 and 8, it can be seen that increasing $|C_w|$ causes an increase in the magnitude of Nu.

Fig 9 shows the results for $C_w = -3000$, $Re_\phi = 1.5 \times 10^6$, $\lambda_T = -0.034$: the flow rate is the same as for Fig 8 but the rotational speed is higher. Again, it can be seen that the computed values of Nu exhibit the experimental trends but tend to underestimate the magnitude of Nu at the larger values of x.

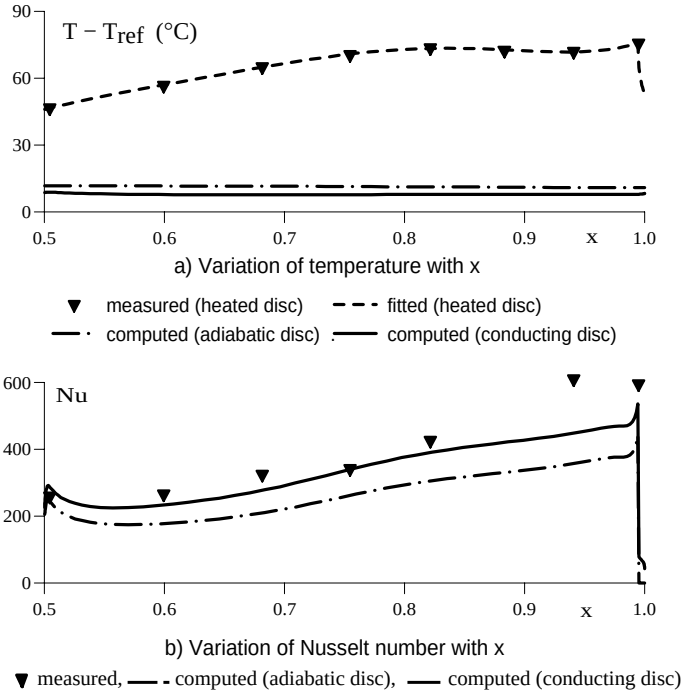

Fig. 8 Variation of temperatures and Nusselt numbers with x: $C_w = -3000$, $Re_\phi = 3.75 \times 10^5$, $\lambda_T = -0.104$

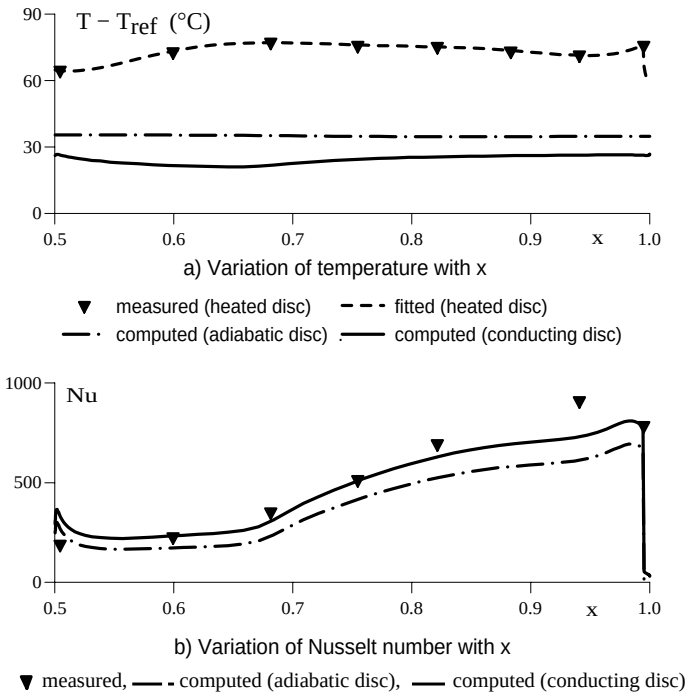

Fig. 9 Variation of temperatures and Nusselt numbers with x: $C_w = -3000$, $Re_\phi = 1.5 \times 10^6$, $\lambda_T = -0.034$

Considering Figs 6 to 9 as a whole, the following conclusions can be drawn. The magnitude of Nu increases as Re_ϕ and $|C_w|$ increase. The computed values of Nu for the conducting-disc case are in better agreement with the experimental data than those for the adiabatic-disc case. The computed values show variations of Nu with x, C_w and Re_ϕ similar to those shown by the experimental data, but the computed values tend to underestimate the measured values, particularly at the larger values of x. A possible reason for this underestimate of Nu is that the measurements were made with a "rough" casing (see Section 2), and the effects of roughness were not modelled in the computations.

5 CONCLUSIONS

A combined computational and experimental study of the flow and heat transfer in a rotating cavity with a peripheral inflow and outflow of cooling air has been conducted for rotational Reynolds numbers up to $Re_\phi = 1.5 \times 10^6$ and flow rates up to $|C_w| = 3000$.

The measured values of $V_\phi/\Omega r$ show a Rankine-vortex behaviour that is not accurately captured by the computations. The use of a "Richardson correction" in the Launder-Sharma low-Reynolds-number k-ε turbulence model improves the agreement between the computed and measured values of $V_\phi/\Omega r$.

The measured and computed values of $V_r/\Omega r$ confirm the recirculating nature of the flow, with radial outflow in the boundary layers on the disc and inflow in the core between the boundary layers. Agreement between computations and measurements in the outflow region is mainly good, but the computations exhibit a "peaky" distribution in the inflow region that is not shown in the measurements. This peaky distribution is attributed to the axisymmetric assumption made in the computations and to possible deficiencies in the turbulence model.

The measured and computed Nusselt numbers show that Nu increases as Re_ϕ and $|C_w|$ increase. The computed Nusselt numbers show the measured trends but tend to underestimate the measured values of Nu at the larger values of x. A possible reason for this underestimate is that the inner and outer cylindrical surfaces of the experimental rig were rough (which affected the tangential component of velocity) and this roughness was not allowed for in the numerical model. Deficiencies in the turbulence model, referred to above, may also have contributed to the underestimates of Nu.

ACKNOWLEDGEMENTS

The authors wish to thank BMW-Rolls Royce GmbH, the UK Engineering and Physical Sciences Research Council and the Defence Research Agency for funding the research described in this paper.

REFERENCES

Chen, J. X., Gan, X. and Owen, J. M. 1995 Heat transfer from air-cooled contra-rotating discs, ASME Int. Gas Turbine and Aeroengine Cong., Houston, paper 95-GT-184

Gan, X., Mirzaee, I., Owen, J. M., Rees, D. A. S. and Wilson, M. 1996 Flow in a rotating cavity with a peripheral inlet and outlet of cooling air, ASME Int. Gas Turbine and Aeroengine Cong., Birmingham, paper 96-GT-309

Karabay, H. 1996 Radiation heat transfer in a single cavity, internal report, School of Mechanical Engineering, Bath University Report No 60/96.

Kilic, M 1993 Computation of flow between contra-rotating discs, PhD thesis, University of Bath

Owen, J.M. and Rogers, R.H. 1989 Flow and heat transfer in rotating-disc systems, Vol.1: Rotor-stator systems. Research Studies Press, Taunton UK and John Wiley, New York, USA

Owen, J.M. and Rogers, R.H. 1995 Flow and heat transfer in rotating disc systems: Vol. 2: Rotating cavities. Research Studies Press, Taunton, UK and John Wiley, New York, USA

Sloan, D. G., Smith, P. J. and Douglas Smoot, L. 1986 Modelling of swirl in turbulent flow systems, Prog. Energy Combust. Sci., v 12, pp 163-250

Wilson, M., Pilbrow, R and Owen, J.M. 1995 Flow and heat transfer in a pre-swirl rotor-stator system. ASME Int. Gas Turbine and Aeroengine Cong., Houston, paper 95-GT-239

APPENDIX A Richardson-number correction to the Launder-Sharma k-ε turbulence model

For cases of combined free and forced vortex flow, Richardson-number based corrections have been proposed for the source term in the ε equation of the k- ε turbulence model, and several formulations have been reported in the literature (see Sloan et al (1986)) for different flow situations. In the present work, following testing of a number of previously-proposed modifications, a gradient Richardson number for swirl, defined as:

$$Ri_{gs} = \frac{k^2}{\varepsilon^2}\frac{V_\phi}{r^2}\frac{\partial}{\partial r}\left(rV_\phi\right) \qquad (A1)$$

was used to modify a source term coefficient in the transport equation for ε as follows:

$$C_{\varepsilon 2,\mathrm{eff}} = C_{\varepsilon 2}\left(1 - C_{gs}Ri_{gs}\right) \qquad (A2)$$

For the present study, the value of the coefficient C_{gs} was optimised numerically, and a value C_{gs}=0.7 was obtained. In the basic model C_{gs} = 0; C_{e2} = 1.92 is the value usually taken for this empirical coefficient. In the modified model, the variation of the coefficient using equation (A2) was constrained by $0.1 < C_{e2,\mathrm{eff}} < 2.4$ (Sloan et al (1986)).

APPENDIX B Conduction model for the unheated disc

For steady flow, the heat flux q through the unheated disc was written as (see Fig. B1):

$$q = h_{TOT}(T_W - T_E) = k_{air}\,(dT/dz)_W \qquad (B1)$$

where h_{TOT} is the total heat transfer coefficient, defined by:

$$h_{TOT} = \frac{1}{\frac{\Delta Z_{DISC}}{k_{DISC}} + \frac{1}{h_{EXT}}} \qquad (B2)$$

The heat transfer coefficient at the exterior disc surface, h_{EXT} (Fig. B1), was deduced from the relationship $Nu=0.015Re_\phi^{0.8}$, for heat transfer from an isothermal free disc into air (see Owen and Rogers, 1989). The values of ΔZ_{disc} and k_{disc} were taken as 10 mm and 0.2 W/mK respectively.

The temperature gradient at the interior wall (in equation (B1)) was expressed using a second order formula involving the interior surface temperature, T_w, and computed fluid temperatures (Kilic, 1993). Equation (B1) was then solved to give the interior wall temperature of the unheated disc, with the exterior temperature T_E taken to be the same as that of the cooling air at inlet.

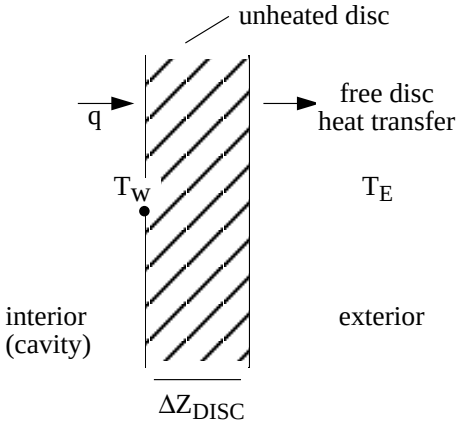

Fig. B1 Conduction model definition sketch